Rafał BIAŁEK

Military University of Technology, Faculty of Electronics

doi:10.15199/48.2020.12.31

Laboratory stands for generating an alternating magnetic field

***Abstract**. The research paper reviews two laboratory stands, based on a Helmholtz coil, for generating an alternating magnetic field. The first stand enables generating an alternating magnetic field of any shape and frequency up to 26 Hz. The task of the second one is to generate an attenuated harmonic signal, with a fundamental frequency of 7.7 kHz. The article also presents a time waveform of the generated magnetic field.*

***Streszczenie.** W pracy przedstawiono dwa stanowiska laboratoryjne do generowania zmiennego pola magnetycznego, oparte na cewce Helmholtza. Stanowisko pierwsze umożliwia generowanie zmiennego pola magnetycznego o dowolnym kształcie i częstotliwości do 26 Hz. Zadaniem drugiego stanowiska jest wytwarzanie sygnału harmonicznego tłumionego o częstotliwości podstawowej 7,7 kHz. W artykule przedstawiono postać czasową generowanego pola magnetycznego (**Stanowiska laboratoryjne do generowania zmiennego pola magnetycznego**).*

Keywords: Magnetic field source, Helmholtz coil, magnetic field
Słowa kluczowe: Źródło pola magnetycznego, cewka Helmholtza, pole magnetyczne

Introduction

The research paper presents two stands for generating an alternating magnetic current, which are based on the Helmholtz coil. The stands were used to conduct tests on a magnetic field sensor reviewed in the publication [1]. The specific shape of the time waveform of the magnetic field strength was obtained through coil current control. The magnetic field strength generated by the Helmholtz coil [2] is expressed by the following formula:

$$H = \left(\frac{4}{5}\right)^{\frac{3}{2}} \cdot I \cdot \frac{N}{R} \tag{1}$$

where: I - current, N - number of coil windings, R - coil radius.

Stand 1

Figure 1 shows a block diagram of a stand for generating an alternating magnetic field of any shape.

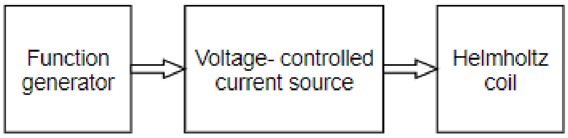

Fig. 1. Block diagram of laboratory stand 1

View of a finished laboratory stand is shown in Fig. 2.

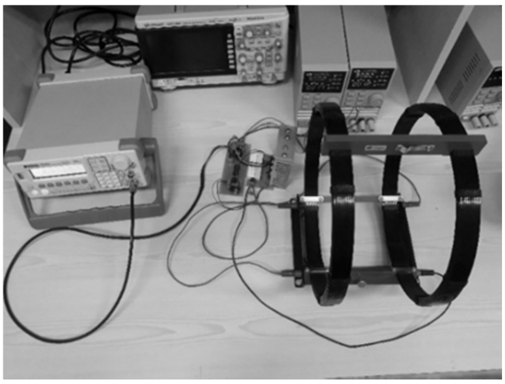

Fig. 2. Laboratory stand 1

The basic element of laboratory stand 1 is the voltage-controlled current source, executed based on a schematic diagram shown in the paper [3]. The execution of the system was preceded by computer simulations in the *Multisim* environment by *National Instruments*. The tests involved determining the transfer characteristic, frequency characteristic and system response to selected inputs. The correct functioning of a voltage-controlled current source within the simulation software contributed to the construction of the actual system (Fig. 3).

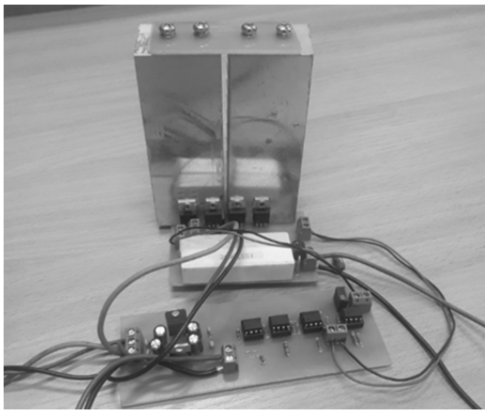

Fig. 3. Constructed voltage-controlled current source

Relation between the coil current and input voltage is shown in Figure 4.

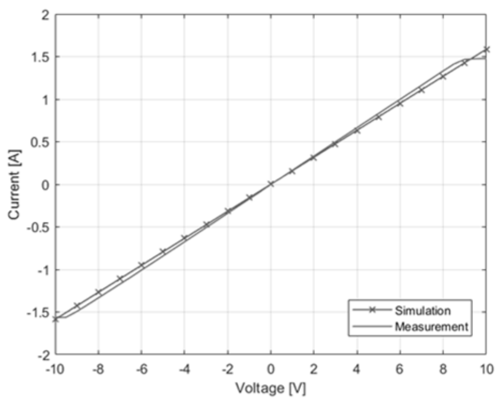

Fig. 4. Relation between the coil current and input voltage

The coil current flowing through the coil is consistent with the relationship:

$$I_L = \frac{Vin}{6,3} \tag{2}$$

Relationship between the coil current and frequency is shown in figure 5.

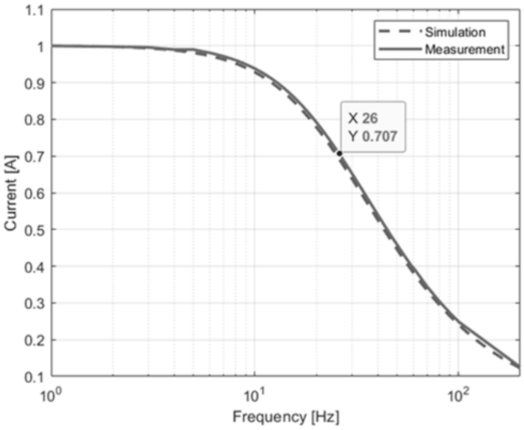

Fig. 5. Relationship between the coil current and frequency

Figure 6 shows the system response to excitation through a sinusoidal signal with a frequency of 5 Hz and an amplitude of 6.3 V in the *Multisim* software.

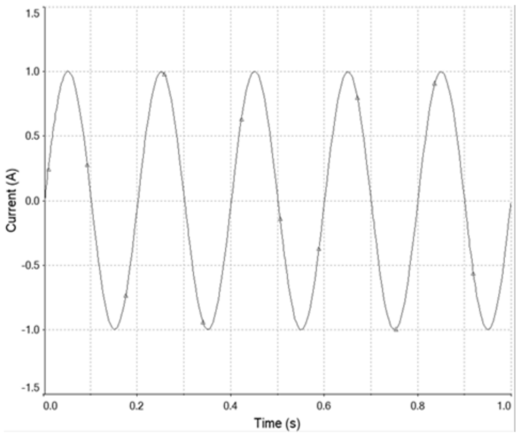

Fig. 6. Time simulation results for excitation with a sinusoidal signal

Figure 7 shows the system response to excitation with a triangle signal with a frequency of 5 Hz and an amplitude of 6.3 V.

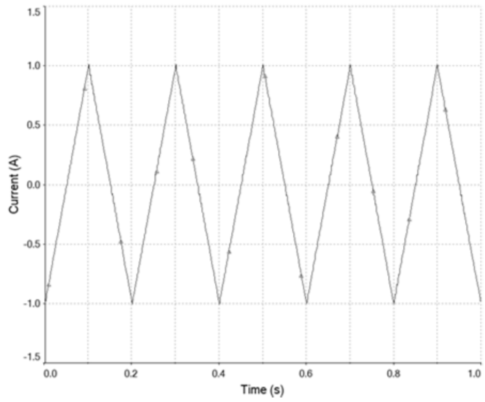

Fig. 7. Time simulation results for excitation with a triangle signal

Then, the authors conducted similar measurements of the current flowing through the coil in an actual circuit. A 1146A current probe by Hewlett Packard was used for this purpose. The measurement results are shown in figures 8 and 9.

The conducted measurements indicate that the current amplitude value is slightly different than in the simulation program, however the signal shape corresponds to the excitation

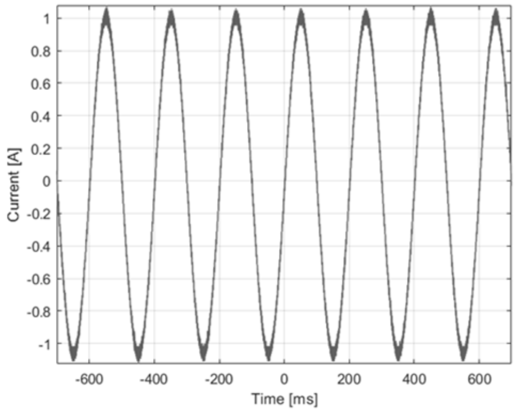

Fig. 8. Current measurement results for sinusoidal signal excitation

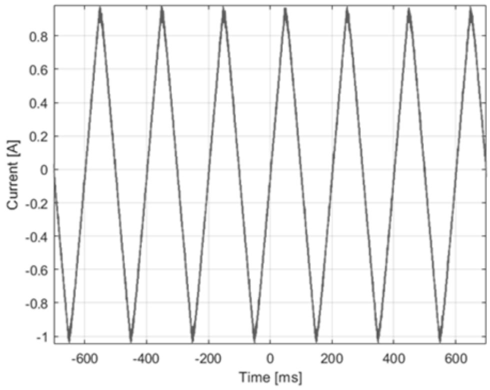

Fig. 9. Current measurement results for triangle signal excitation

Stand 2

The basic task of the second stand was generating an attenuated sinusoidal signal with a fundamental frequency of approx. 7.7 kHz. The schematic diagram of the system is shown in Figure 10.

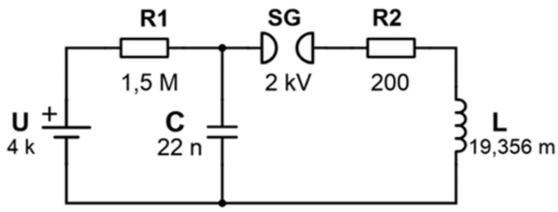

Fig. 10. Schematic diagram of a system for generating an attenuated sinusoidal signal

The diagram does not take into account the Helmholtz coil resistance, since it has a negligible impact on the time waveform of the pulse signal. High-voltage source constructed by the author of the paper enables generating a voltage of 4 kV. The capacitor C is charged by a resistor R1. Reaching a voltage of 2 kV results in an electric breakdown at the spark gap SG and a sudden drop in its resistance [4]. Therefore, attenuated sinusoidal oscillations appear within the Helmholtz coil. These oscillations are generated during the arc discharge. The time waveform of the current flowing through the coil is consistent with the relationship [5]:

$$i(t) = \frac{U_{break}}{2\pi \cdot f \cdot L} \cdot sin(2 \cdot \pi \cdot f \cdot t) \cdot e^{-\beta \cdot t} \quad (3)$$

where: U_{break}- breakthrough voltage value, L - Helmholtz coil inductance, f - oscillation frequency, β - attenuation factor.

The frequency of attenuated oscillations in such a system is consistent with the relationship:

(4) $$f = \frac{1}{2\pi}\sqrt{\frac{1}{L \cdot C} - \beta^2}$$

The attenuation factor value is expressed as:

(5) $$\beta = \frac{R2}{2 \cdot L}$$

An analysis in the Multisim software by National Instruments was conducted in order to verify the correct functioning of the system. The spark gap was replaced by a key S1. For the time of the simulation, it was assumed that the closing moment occurs when the voltage in the capacitor reaches a value of 2 kV. This time was determined based on the relationship:

(6) $$t = -\ln\left(\frac{U_{break}}{U}\right) \cdot \tau$$

where: U - HV generator voltage value, τ - R1C circuit time constant.

System diagram in the Multisim software is shown in Fig. 11.

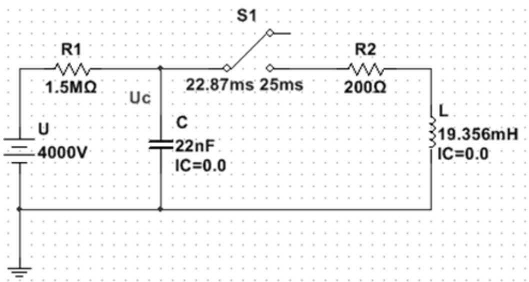

Fig. 11. Diagram of the system in the *Multisim* software

The time analysis was conducted for a range from 0 to 25 ms, with an increment of 1 μs. Figure 12 shows the voltage waveform in the capacitor and of the current in the coil.

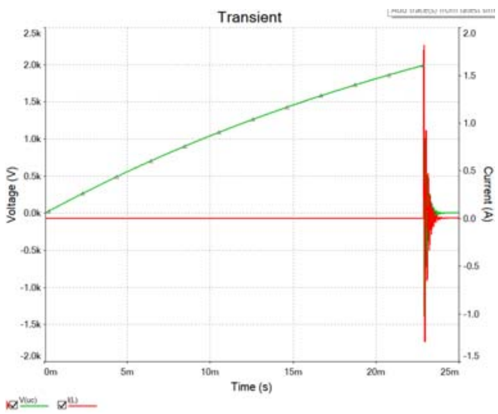

Fig. 12. Transient simulation in the *Multisim* software

Figure 13 shows the signal over a time interval, in which attenuated harmonic oscillations occur. The current amplitude and frequency in the coil were measured using the cursor method.

The conducted simulation shows that the current amplitude is approx. 1.8 A and the frequency of generated oscillations is equal to approx. 7.7 kHz. The stand enabling the generation of a pulse signal is shown below.

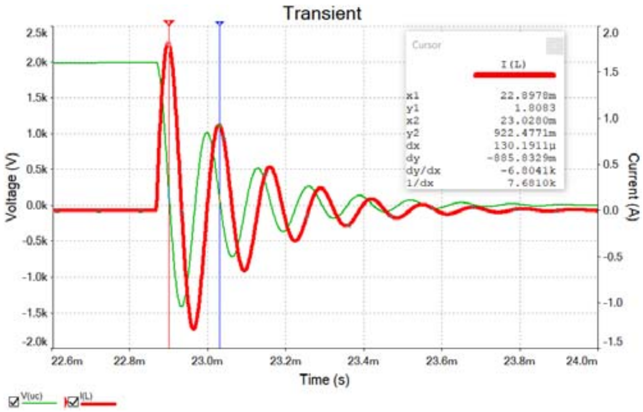

Fig. 13. Waveform of voltage in the capacitor and of the current in the coil.

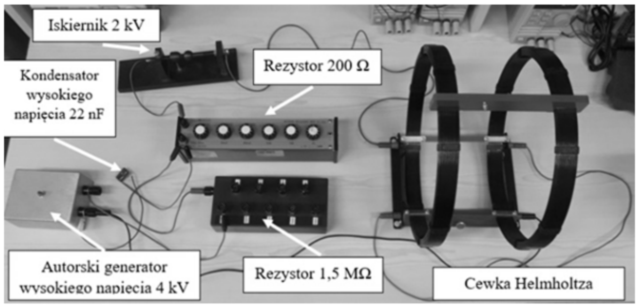

Fig. 14. Stand for generating an attenuated sinusoidal signal with a fundamental frequency of 7.7 kHz.

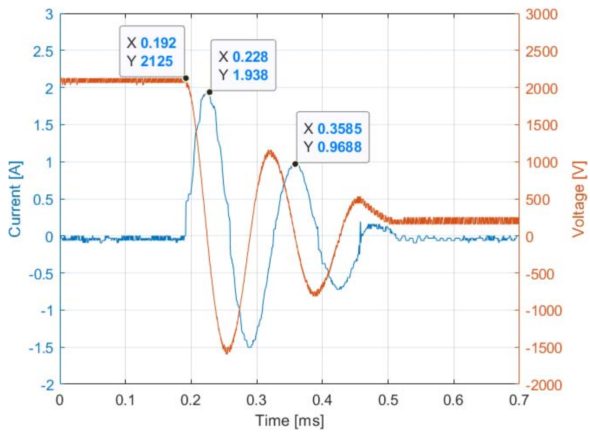

Fig. 15. Voltage in the capacitor and current in the Helmholtz coil

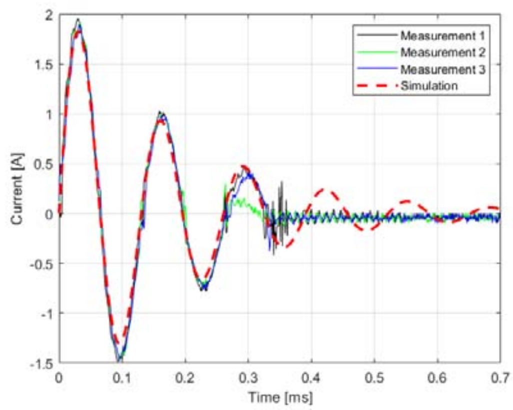

Fig. 16. Current in the Helmholtz coil

In order to verify the functionality of the system, the voltage in the capacitor and the current flowing through the coil were measured using a TT-HVP 15HF high-voltage probe by Testec and a 1146A current probe by Hewlett Packard. An example of a waveform is shown in Figure 15.

Figure 16 shows the simulation current waveform with the waveform recorded over three consecutive attempts.

Recorded waveforms confirm the correct functioning of the system. However, the oscillation duration is limited by the spark gap conduction time. The recorded waveforms, the first two in three subsequent trials in particular, are characterized by high repeatability.

Magnetic field strength measurement results

The magnetic field strength was measured using a 5080 meter by Sypris Test & Measurement. Figure 17 shows a magnetic field strength signal for a sinusoidal signal excitation with an amplitude of 6.3 V and a frequency of 5 Hz, obtained using stand 1.

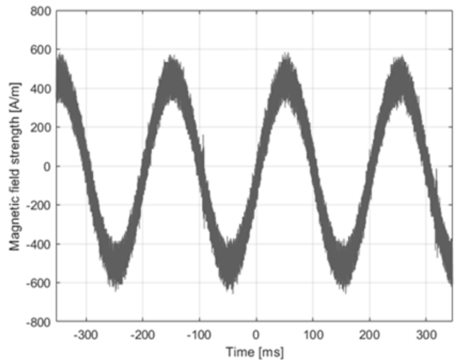

Fig. 17. Magnetic field strength for a sinusoidal excitation

Figure 18 shows a magnetic field strength signal for a triangle signal excitation with an amplitude of 6.3 V and a frequency of 5 Hz, obtained using stand 1.

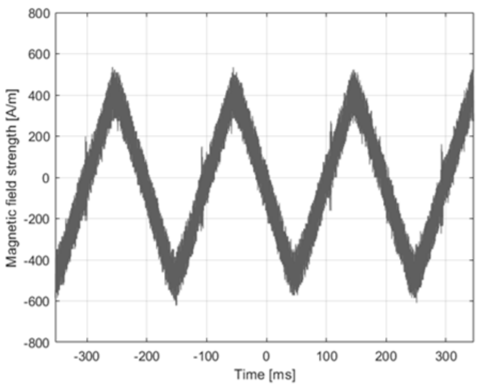

Fig. 18. Magnetic field strength for a triangle excitation

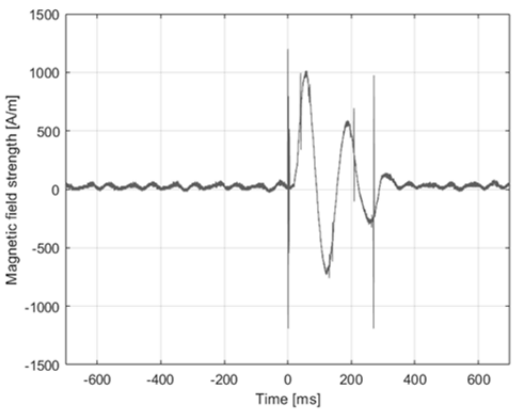

Fig. 19. Signal generated by stand 2

Figure 19 shows a magnetic field strength signal obtained using stand 2.

Conclusions

Two laboratory stands for generating an alternating magnetic field were used within this research work.

The first stand enables generating low-frequency signals, with their spectrum containing components with frequencies up to 26 Hz. The shape and parameters of the generated magnetic field depend on the control signal parameters, declared on the functional generator.

The second stand enables generating a pulse waveform with a fundamental frequency of 7.7 kHz. The change in the generated frequency and attenuation factor can be achieved through changing the value of the capacitance C and resistance R2.

***Authors**:*
mgr inż. Rafał Białek, Military University of Technology, Institute of Electronic Systems, ul. Gen. Sylwestra Kaliskiego 2, 00-908 Warsaw, E-mail: rafal.bialek@wat.edu.pl.

REFERENCES

[1] R. Białek, M. Wiśnios, and M. Kuchta, “Badania prototypowego detektora pola magnetycznego, w szczególności impulsów HPEM”, *Przegląd Elektrotechniczny*, vol. 95, no. 12, pp. 93–96, 2019,

[2] C. F. de Melo, R. L. Araújo, L. Morozowski Ardjomand, N. S. Ramos Quoirin, M. Ikeda and A. A. Costa, “Calibration of magnetic field meters at 60 Hz using a Helmholtz coil: constructive aspects and calculation of associated uncertainties”, *XVIII IMEKO WORLD CONGRESS Metrology for a Sustainable Development*, Rio de Janeiro, Brazil, September, 2006

[3] P. Oxley, “Apparatus for magnetization and efficient demagnetization of soft magnetic Materials”, IEEE Transactions on Magnetics, vol. 45, no. 9, pp. 3274-3283, 2009,

[4] X. Li, X. Liu, F. Zeng, H. Yang and Q. Zhang, "Study on Resistance and Energy Deposition of Spark Channel Under the Oscillatory Current Pulse," in *IEEE Transactions on Plasma Science*, vol. 42, no. 9, pp. 2259-2265, Sept. 2014, doi: 10.1109/TPS.2014.2331346.

[5] R. I. Kurhade, A. Sharma and P. C. Saroj, "Trigger generator for spark gap switching synchronisation," *2017 Innovations in Power and Advanced Computing Technologies (i-PACT)*, Vellore, 2017, pp. 1-5, doi: 10.1109/IPACT.2017.8245031.